



Growth, Structure, Spectral Characterization, Fluorescence and Thermal Studies on Phenyltrimethylammonium Trichloro Cadmate (II) Crystals

V. Mohanraj^{1*}, M. Thenmozhi³, R. Pavithra², Jaslin J. Christopher¹, A. S. Jebamalar⁴,
R. Umarani²

¹Department of Chemistry, Manonmaniam Sundaranar University Constituents College, Kanniyakumari, TN, India.

²Department of Chemistry, Government Arts College (Autonomous), Coimbatore, TN, India.

³Department of Physics, Bangalore City College, Bangalore, Karnataka, India.

⁴Department of Physics, Nesamony Memorial Christian College, Marthandam, TN, India.

Received : 30.01.2020 Accepted 03.03.2020

Abstract

Crystallography is a fascinating division of the entire study of the optical technology. The single crystal of Phenyltrimethylammonium trichloro cadmate (II) crystals [PTMAC(II)] is grown by slow evaporation technique at room temperature. The grown crystals are characterized using CHN analysis, FT-IR, ¹H NMR spectra to confirm with functional groups and structures in spectroscopy methods. TG/TDA analysis are used to find out the thermal stability of grown crystals and also carry out fluorescence studies. Further, the single crystal X-ray diffraction studies to solve by using SHELXL and refined by full matrix least square methods. The molecule belongs to monoclinic crystal system with C₂/n space group. This work undergoes to phase transition of crystals which makes the study interesting and also inorganic crystals are used for many applications in the field of computer technology.

Keywords: Single crystal X-ray diffraction; FT-IR; ¹H NMR; TG/DTA .

1. INTRODUCTION

Crystal growth is an interdisciplinary subject covering Physics, Chemistry, Material Science, Chemical Engineering, Metallurgy, Geology, Crystallography, Mineralogy and Molecular Biology. Crystals are known to man from the earlier period. Many forms of solid matter are crystalline in nature. Orderly arranged atoms, ions or molecules in crystalline solids provide shining appearance and coloured crystals which are still more attractive. The art of growing crystals has always been fascinating and challenging. Modern technology requires semiconductors, magnetic garnets, solid state lasers, and ultraviolet and infrared requires materials in good crystalline form (Gesi, 1986). Crystals of good quality in suitable size and perfection are required in technologically important fields like electronic industries, computer technologies, fibre optic communications and ferroelectric materials (Fousek, 1991; Ishibashi *et al.* 1986; Sannikov *et al.* 1986). Rapid

advances in microelectronics, communication technologies, medical instrumentations and energy and space technologies are possible simply because of remarkable progress in the fabrication of large and rather perfect crystals (Young Kim *et al.* 1998; Strukov, 1989; Shimomura *et al.* 1995; Asahi and Hasebe, 1994; Hasebe *et al.* 1994; Heine and Mc Connel, 1984). Crystals are pillars of modern technology. If there is no crystal, there would be no electronic industry, photonic industry, and fibre optic communications (Kasano *et al.* 1992; Dvorak and Kind, 1981; Kahirizi and Steinitz, 1989). Crystals have an important role in the production of highly effective light emitting diodes. Energy saving illumination and photovoltaic devices for transforming solar and other radiation into electric power with high yield depend on significant advances in crystal growth (Sato *et al.* 1986; Ganguly *et al.* 1985; Kapustianik *et al.* 1995; Sawada *et al.* 1978; Mashiyama *et al.* 1980). The significance of the beauty of crystals for a technological society and the development of scientific knowledge has

*Dr. V Mohanraj

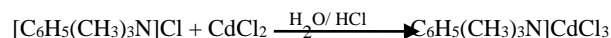
email:chemistrymohan@gmail.com

been realized. The inorganic and organic crystals are differing in fundamental way from gases, liquids and solids. The grown crystals with more components have an important role in several industrial and optical applications (Mohanraj *et al.* 2019a; 2019b). Fluorescence compounds are widely useful in chemico-physico sensors and fluorescent labeling. Phenyl groups are excellent chromospheres and their metal complexes show strong lights emitting properties and fluorescence for long durability (Subashini and Arjun, 2018; Peer Mohamed *et al.* 2019).

2. EXPERIMENTAL

Single crystals of Phenyltrimethylammonium trichloro cadmate (II) [PTMATCl-Cd (II)] crystals are grown by slow evaporation method at room temperature. The compound is prepared by mixing phenyltrimethylammonium chloride and cadmium chloride in 1:1 molar ratio using triply distilled water as the solvent. The two solutions are mixed thoroughly. In order to maintain acidic medium and to avoid hydrolysis, 1 ml of HCl is added. The resulting solution is filtered using the Whatmann paper 42. The filtrate collected in a beaker is covered by a filter paper with minute pores and kept at room temperature for the preparation of crystal by slow evaporation. The crystals obtained are colourless and transparent.

The compound was obtained according to the following chemical equation:



Phenyltrimethylammonium trichloro cadmate (II) Crystal

3. RESULTS & DISCUSSION

3.1 Elemental Analysis

The result of elemental analysis (C, H and N) of crystals and the comparison of theoretical values and experimental values are given in the Table 1. The experimental values of Carbon, Hydrogen and Nitrogen are very close to the theoretical values based on ABX₃ formula. The elemental analysis thus confirms the stoichiometry of the PTMATCl-Cd(II) compound. This technique is used to find out Carbon, Hydrogen, Nitrogen elements' percentage and other elements are calculated.

Table 1. CHN Analysis of PTMATCl – Cd(II) crystals

Sample Name	Carbon %		Hydrogen %		Nitrogen %	
	Exp	Theo	Exp	Theo	Exp	Theo
PTMACl - Cd[II]	30.40	30.42	4.19	3.94	3.94	3.94

3.2 FT-IR Spectrum

The FTIR spectra of PTMATCl-Cd(II) is shown in the fig. 1. The various absorption frequencies and their assignments are present in the Table 2. The peak at 3044.32 cm⁻¹ is due to Ar-H stretching vibrations of phenyl group. The peak at 1594.91 cm⁻¹ is due to C-N bending mode. The peak at 1490.57 cm⁻¹ is due to C-H in-plane asymmetric bending due to methyl group. The peak at 1460.70 cm⁻¹ is due to C-H bending deformation mode of methyl group. The peak at 949.61 cm⁻¹ is due to C-H out of plane bending vibration. The peak at 843.61 cm⁻¹ is due to C-H deformation out of plane vibration. The peak at 757.44 cm⁻¹ is due to aromatic in-plane bending vibration and metadisubstituted aromatic ring stretching. This region helps to identify the type of substitution on aromatic ring. C-N-C and C-C-N deformation modes, disubstituted meta C-H deformation are seen at 685.50 cm⁻¹.

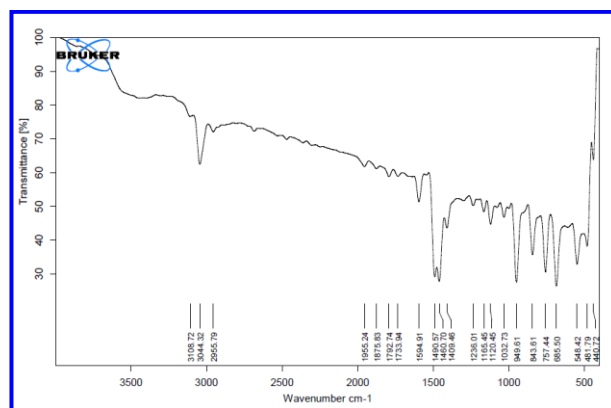


Fig. 1: FTIR Spectrum of PTMATCl-Cd(II) crystals

Table 2. FTIR spectral data for PTMATCl – Cd(II) crystals

S. No.	Frequency (cm ⁻¹)	Assignment
1.	3044.32	Ar-H stretching vibrations of phenyl group.
2.	1594.91	C-N bending mode.
3.	1490.57	C-H in-plane asymmetric bending due to methyl group
4.	1460.70	C-H bending deformation mode of methyl group
5.	949.61	C-H out of plane bending vibration
6.	843.61	C-H deformation out of plane vibration
7.	757.44	Aromatic in-plane bending vibration, meta disubstituted aromatic ring stretching
8.	685.50	C-N-C and C-C-N deformation modes.

Therefore, IR spectral analysis of PTMATPCI-Cd (II) confirms the presence of fundamental groups of various bonding vibration of the compound. The Cd-Cl bond is a weak bond vibration and hence these frequencies occur in the Far IR region.

3.3 ^1H NMR Spectroscopy

The normal ^1H NMR spectrum of PTMATCI-Cd (II) crystals is shown in the fig.2. The structure of PTMATCI-Cd [II] compound is $\text{C}_6\text{H}_5(\text{CH}_3)_3\text{NCdCl}_3$. In this spectrum, four signals are observed at different δ values for the methyl and Ar-H groups are present in the compound. All the methyl and Ar-H groups are in the same environment. The expected δ values for methyl and aromatic protons are 1.2 to 1.4 ppm and 7.5 to 7.8 ppm. In this spectrum, higher δ value is obtained. This is due to the deshielding effect which confirms the presence of positive charge on the nitrogen containing three methyl groups and Ar-H groups. The signal at 3.6 δ is due to the presence of methyl group protons. The intensity of the peak is higher due to methyl proton. The peak at 7.9 δ is due to Ar-H protons and it splits into a triplet. The peak at 7.9 δ splits into a triplet due to an aromatic proton. The peak at 7.6 δ splits into a triplet due to an aromatic proton.

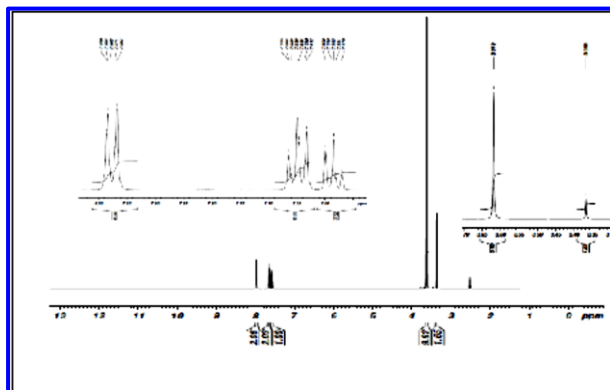
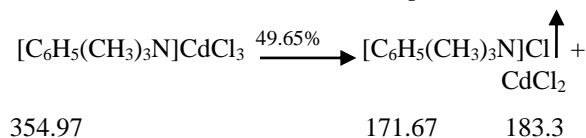


Fig. 2 ^1H NMR Spectrum of PTMATCI-Cd(II) crystals

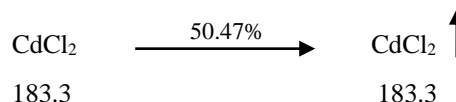
3.4 Thermogravimetry-Differential Thermal Analysis (TG-DTA)

The TG-DTA thermogram of the compound phenyltrimethylammonium trichloro cadmate(II) crystals is shown in the fig. 3. The compound is subjected to uniform heating of $20^\circ\text{C} / \text{minute}$ in nitrogen atmosphere. The TG-DTA curve showed a two stage weight loss when heated between the room temperature and 800°C . The first stage decomposition started at 180°C and ended at 536°C . There is a weight loss of 49.63% which can be accomplished by

formulating the following decomposition reaction of the compound. When the compound undergoes decomposition as above, one mole of the compound decomposes into one mole of phenyltrimethylammonium chloride and one mole of cadmium chloride. Since $[\text{C}_6\text{H}_5(\text{CH}_3)_3\text{N}]\text{CdCl}_3$ is stable at these temperatures, it does not vaporize at these temperatures. The theoretical loss of 49.63 % is observed whereas the experimental loss observed is 48.36%. The difference is 1.29 % which indicated the experimental and theoretical values are close to each other and the result was within the experimental error.



In the second stage, there is only one mole of cadmium chloride that decomposes at 524°C . When the temperature is increased, there is decomposition of CdCl_2 from 524°C to 699°C with a weight loss of 50.47%. This weight loss can be accounted for by formulating the following reaction.



The experimental weight loss is 50.47%. But the theoretical weight loss is 51.6%. The difference is 1.13% which indicated the experimental and theoretical values are close to each other and the result was within the experimental error. The theoretical residual mass is 0.1%. Experimentally, there is no residue. Thus the compound decomposes in two stages. The decomposition starts at 180°C and gets completed at 700°C . Thus the thermogram confirms the stoichiometry of the compound which is evident from the decomposition patterns.

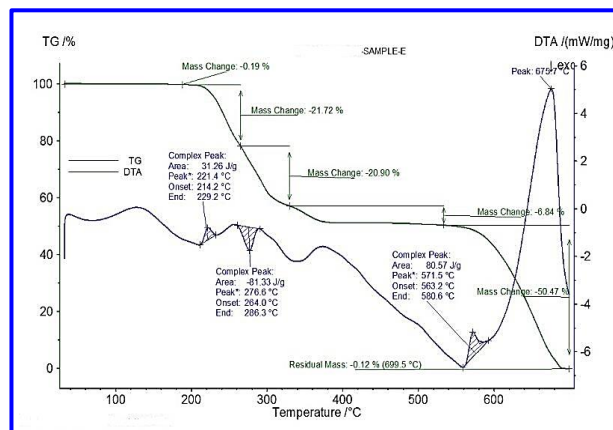


Fig. 3: TG-DTA spectrum of PTMATCI-Cd(II) crystals

3.5 Fluorescence studies

The emission of the light which dwindles due to the excitation in cut-off is due to fluorescence. Fluorescence is a physico-chemical property which occurs in molecules that are aromatic compounds and contains multiple conjugated double bonds with a high degree of resonance stability. The Fluorescence spectrum of PTMATCI-Cd (II) crystal was measured to confirm the emission spectrum concerned with that particular excited state of the system. The Fluorescence emission spectrum of PTMATCI-Cd (II) crystal is shown in the fig. 4. The observed emission peak with maximum intensity at 534 nm shows that the crystal exhibits green colour fluorescence emission. Also the existence of only one sharp peak indicates the good crystalline perfection.

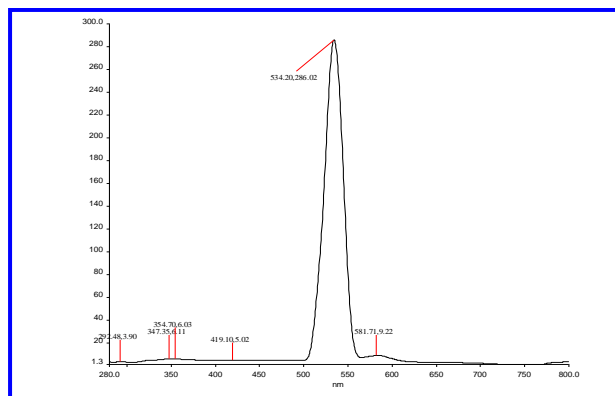


Fig. 4: Fluorescence spectrum of PTMATCI-Cd (II) crystals

3.6 Single crystal X-ray structural analysis of PTMATCI-Cd (II) Crystals

The structure of the compound is determined by single crystal X-ray diffraction technique. The X-ray data for the compound are collected at 293K using the M_oK_{α} radiation ($\lambda = 0.71073 \text{ \AA}$). The unit cell parameters of the crystal are determined by least square using several reflections. The structure is solved by using SHELXL and refined by full matrix least square method. The intensity data are collected for $h = -16$ to 17 , $k = -14$ to 19 , $l = -9$ to 9 . The crystal structure data for the grown crystal is present in the Table 3.

The C-N-C bond angles are given in the Table 3. There is no greater deviation when the bond angles are around the normal tetrahedral angle of 109.5° . In some cases observed from the Tables 2-11, the bond angles are less than the normal tetrahedral angle while in some other cases. The bond angles are greater than the normal tetrahedral angle which indicates that there is a steric and electronic strain around these groups.

Table 3. Crystal structure data of PTMATCI – Cd(II) crystals

Empirical formula	$C_9H_{14}CdCl_3N$
Formula weight	354.96
Temperature	293(2) K
Wavelength	0.71073 Å
Unit cell dimensions	$a = 12.7634(3) \text{ Å}$ $\alpha = 90^\circ$ $b = 14.4964(5) \text{ Å}$ $\beta = 96.375(5)^\circ$ $c = 7.1365(7) \text{ Å}$ $\gamma = 90^\circ$ $\alpha = \gamma = 90^\circ, \beta \neq 90^\circ$
Space group	P21/n
Crystal system	Monoclinic
Volume	$1312.25(14) \text{ Å}^3$
Z, Calculated density	4, 1.797 Mg/m^3
Absorption coefficient	2.239 mm^{-1}
F(000)	696
Theta range	2.13 to 28.49°
Limiting indices	$-16 \leq h \leq 17$ $-14 \leq k \leq 19$ $-9 \leq l \leq 9$
Reflections collected / unique	6080 / 2733 [R(int) = 0.0328]
Completeness to theta = 25.00°	99.90%
Refinement method	Full-matrix least-squares on F^2
Data / restraints / parameters	2733 / 2 / 130
Goodness-of-fit on F^2	1.06
Final R indices [I > 2sigma(I)]	$R1 = 0.0697$, $wR2 = 0.2041$
R indices (all data)	$R1 = 0.0706$, $wR2 = 0.2057$
Absolute structure parameter	0.09(9)
Largest diff. peak and hole	5.987 and -1.600 e.Å^{-3}

Table 4. Bond angles for C-N-C

Group	Bond angle ($^\circ$)
C(9)-N(1)-C(6)	110.9(10)
C(9)-N(1)-C(7)	111.0(11)
C(6)-N(1)-C(7)	109.3(10)
C(9)-N(1)-C(8)	107.2(13)
C(6)-N(1)-C(8)	111.7(11)
C(7)-N(1)-C(8)	106.8(13)

Table 5. Bond angles for H-C-H

Group	Bond angle ($^\circ$)
-------	-------------------------

H(7A)-C(7)-H(7B)	109.5
H(7A)-C(7)-H(7C)	109.5
H(7B)-C(7)-H(7C)	109.5
H(8A)-C(8)-H(8B)	109.5
H(8A)-C(8)-H(8C)	109.5
H(8B)-C(8)-H(8C)	109.5
H(9A)-C(9)-H(9B)	109.5
H(9A)-C(9)-H(9C)	109.5
H(9B)-C(9)-H(9C)	109.5

In majority of the H-C-H groups, the tetrahedral angle observed is exactly 109.5° which indicates the ideal tetrahedral nature of the bonds in all these groups. These groups are not at all affected by any strain present in the compound. In the case of some other H-C-H groups, the deviation is very minimum showing again the tetrahedral nature of the groups. The bond angles suggest that all the bond angles are nearly tetrahedral. The C-C-N bond angles are given in the Table 6. The variation in the bond angles are due to varying degrees of steric and electronic repulsions around the phenyl group in the positive ion. Also, the nitrogen is positively charged and the N-C bond is not completely covalent in nature. From the Table 7, it is very clear that the C-C-C bond angles are nearly tetrahedral in many of the C-C-C groups. In certain cases, there is an increase in the bond angle. For C(4)-C(3)-C(2), the bond angle is 121° . This increase from the normal tetrahedral angle is attributed to steric and electronic repulsion around these groups from the bond angles shown in the Table 8. It is very clear that all the bond angles are nearer to the normal tetrahedral angle of 109.5° . Hence it is obvious that there is no distortion in the tetrahedral symmetry of the C-C-H groups. In the CdCl_3 tetrahedral group, a bond length of 2.429\AA to 2.847\AA is observed for all the Cd-Cl bonds. The Cd-Cl bond length is greater than C-H, C-N and C-C bond lengths. The hydrogen bonds present between the hydrogen of the methyl group and chlorine of the CdCl_3 group lead to a stronger interaction between the Ar-N and CdCl_3 . The structure of cobalt compound is $[\text{C}_6\text{H}_5(\text{CH}_3)_3\text{N}]\text{CdCl}_3$. From the Table 8, it is very clear that all the C-C bonds have more or less the ideal bond length. The very small differences may be due to the strain in their environment. The C-H bond length in phenyl groups are 0.93 while it is 0.96 for all the methyl groups. From the Table 11, it is clear that the C-N bond length is more or less same for all the groups. The expected C-N bond length is seen in all the cases. In the CdCl_3 tetrahedra group, a bond length of 2.429\AA to 2.847\AA is observed for all the Cd-Cl bonds in the Table

12. Usually, the metal-halogen bonds are weaker and hence the bond length is higher. The Cd-Cl bond length is greater than C-H, C-N and C-C bond lengths. The hydrogen bonds present between the hydrogen of the methyl group and chlorine of the CdCl_3 group lead to a stronger interaction between the Ar-N and CdCl_3 . The structure of the title compound is $[\text{C}_6\text{H}_5(\text{CH}_3)_3\text{N}]\text{CdCl}_3$ as shown in the fig. 5 and also ORTEP plot structure as given in the fig. 6.

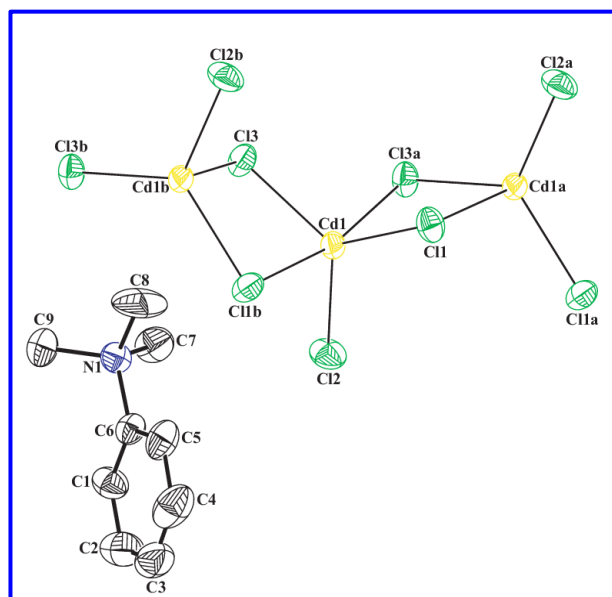


Fig. 5: ORTEP plot of PTMATCl – Cd(II) crystals

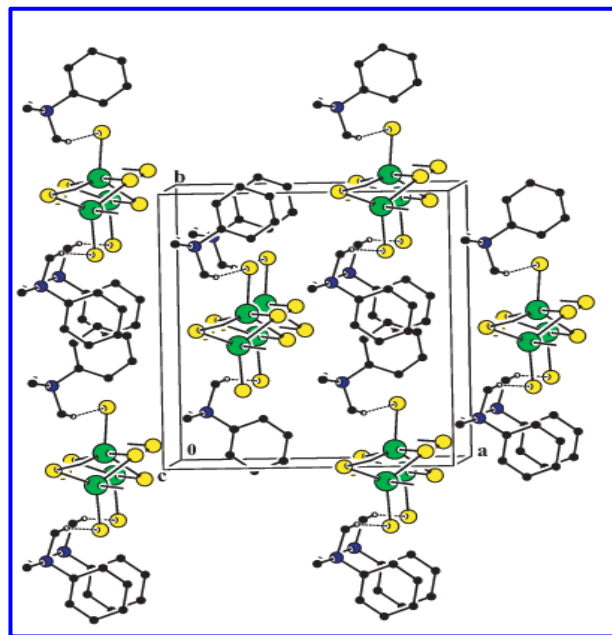


Fig. 6: ORTEP plot of PTMATCl – Cd(II) crystals
Table 6. Bond angles for N-C-H

Group	Bond angle (°)
N(1)-C(7)-H(7A)	109.5
N(1)-C(7)-H(7B)	109.5
N(1)-C(7)-H(7C)	109.5
N(1)-C(8)-H(8A)	109.5
N(1)-C(8)-H(8B)	109.5
N(1)-C(8)-H(8C)	109.5
N(1)-C(9)-H(9A)	109.5
N(1)-C(9)-H(9B)	109.5
N(1)-C(9)-H(9C)	109.5

Table 7. Bond angles for C-C-N

Group	Bond angle (°)
C(1)-C(6)-N(1)	118.4(12)
C(5)-C(6)-N(1)	120.9(12)

Table 8. Bond angles for C-C-C

Group	Bond angle (°)
C(6)-C(1)-C(2)	120.6(17)
C(3)-C(4)-C(5)	120.4(17)
C(4)-C(5)-C(6)	118.5(17)
C(1)-C(6)-C(5)	120.6(14)
C(4)-C(3)-C(2)	121.0(16)

Table 9. Bond angles for C-C-H

Group	Bond angle (°)
C(1)-C(2)-H(2)	120.6
C(2)-C(1)-H(1)	119.7
C(2)-C(3)-H(3)	119.5
C(3)-C(2)-H(2)	120.6
C(3)-C(4)-H(4)	119.8
C(4)-C(3)-H(3)	119.5
C(4)-C(5)-H(5)	120.7
C(5)-C(4)-H(4)	119.8
C(6)-C(5)-H(5)	120.7

Table 10. The Cl-Cd bond distance

Group	Bond angle (°)
C(6)-C(1)-C(2)	120.6(17)
C(3)-C(4)-C(5)	120.4(17)
C(4)-C(5)-C(6)	118.5(17)
C(1)-C(6)-C(5)	120.6(14)
C(4)-C(3)-C(2)	121.0(16)

Table 11. The C-C bond distance

Group	Bond angle (°)
C(6)-C(1)-C(2)	120.6(17)
C(3)-C(4)-C(5)	120.4(17)
C(4)-C(5)-C(6)	118.5(17)
C(1)-C(6)-C(5)	120.6(14)
C(4)-C(3)-C(2)	121.0(16)

Table 12. The C-H bond distance

Groups	Bond Distance (Å°)
C(1)-H(1)	0.93
C(2)-H(2)	0.93
C(3)-H(3)	0.93
C(4)-H(4)	0.93
C(5)-H(5)	0.93
C(7)-H(7A)	0.96
C(7)-H(7B)	0.96
C(7)-H(7C)	0.96
C(8)-H(8A)	0.96
C(8)-H(8B)	0.96
C(8)-H(8C)	0.96
C(9)-H(9A)	0.96
C(9)-H(9B)	0.96
C(9)-H(9C)	0.96

Table 13. The C-N and Cd-Cl bond distance

Group	Bond Distance (°)
C(6)-C(1)-C(2)	120.6(17)
C(3)-C(4)-C(5)	120.4(17)
C(4)-C(5)-C(6)	118.5(17)
C(1)-C(6)-C(5)	120.6(14)
C(4)-C(3)-C(2)	121.0(16)
Group	Bond Distance (°)
Cd(1)-Cl(2)#2	2.429(3)
Cd(1)-Cl(3)#1	2.657(3)
Cd(1)-Cl(1)#3	2.847(3)

4. CONCLUSION

Elemental analysis data obtained for the grown crystal confirmed their molecular formula. The crystalline nature of the prepared compounds from aqueous solution is confirmed by getting well-defined peaks at different 2θ values. The IR spectra were used to assign various vibrational frequencies due to different chemical bonds in these compounds. The IR spectra of all the compounds were similar and confirmed the presence of methyl and methylene groups in these compounds. The ^1H NMR spectra suggested the presence of aromatic and alkyl groups in these compounds. The TG-DTA thermogram indicated 100 % decomposition of the compound. The observed emission peak with maximum intensity at 534 nm shows that the crystal exhibits green colour fluorescence emission. Also the existence of only one sharp peak indicates the good crystalline perfection. The compound $[\text{C}_6\text{H}_5(\text{CH}_3)_3\text{N}]\text{CdCl}_3$ crystallized with needle habits is transparent. The structure of the compound was determined as monoclinic with space group $\text{P}2_1/\text{n}$, the unit cell dimensions of $a = 12.763\text{\AA}$, $b = 14.496\text{\AA}$, $c = 7.136\text{\AA}$ with $Z=4$. The co-ordination around Cd atom is tetrahedral. The structure of the compound also shows hydrogen bonds between chlorine and hydrogen of the phenyl groups. Further, it is concluded that the structure of phenyltrimethylammonium trichloro cadmate (II) crystals are well-defined with the help of the mentioned spectral characterization and materials have more thermal stability in nature. These compounds may be used to optical and industrial applications.

REFERENCES

- Asahi, T. and Hasebe, K., Measurement of monoclinic angle in the ferroelastic phase of $[\text{N}(\text{CH}_3)_4]_2\text{XBr}_4$ ($\text{X}=\text{Zn, Co, Mn, Cd}$), *J. Phys. Soc. Jpn.*, 63(7), 2827-2828(1994).
doi:10.1143/JPSJ.63.2827
- Blinic, R. and Lavanyak, A. P., Incommensurate Phases in Dielectrics : Materials 2, Elsevier Science publisher, 49(1986).
- Dvorak, V. and Kind, R., On the low temperature phase in Rb_2ZnCl_4 , *Physical Status Solid B.*, 107, K109 (1981).
doi:10.1002/pssb.2221070253
- Fousek, J., Birefringence studies of A_2BX_4 compounds with incommensurate phases, *Phase Transitions*, 36(1-4), 165-190(1991).
doi:10.1080/01411599108203438
- Ganguly, S., Raoand, K. J., Rao, C. N. R., *SpectrochimicaActa*, 41B, 307 (1985).
- Gesi, K., Effect of hydrostatic pressure on the phase transitions in tetraethylammonium tetrahalogenometallic compounds, *Ferroelectrics*, 159(1), 49-54(1986).
doi:10.1080/00150199408007547
- Hasebe, K., Mashiyama, H., Tanisaki, S. and Gesi, K., X – Ray study of the phase transitions in $\{\text{N}(\text{CH}_3)_4\}_2\text{ZnBr}_4$ and $\{\text{N}(\text{CH}_3)_4\}_2\text{CoBr}_4$, *J. Phys. Soc. Jpn.*, 53(5), 1866-1868 (1984).
doi:10.1143/JPSJ.53.1866
- Heine, V. and McConnel, J. D., The origin of incommensurate structures in insulators, *J. Physica C*, 17(7), 1199 (1984).
doi:10.1088/0022-3719/17/7/014
- Kahirizi, M. and Steinitz, M. O., A structural phase transitions in $((\text{C}_2\text{H}_5)_4\text{N})\text{CdX}_4$ and $((\text{CH}_3)_4\text{N})_2\text{CdX}_4$ compounds with $\text{X} = \text{Cl, Br}$, *Solid State Communications*, 70(6), 599-603(1989).
doi:10.1016/0038-1098(89)90357-8
- Kapustianik, V., Svelaba, S., Dacko, S., Vajdanych, V. and Mokryi, V., Dielectric properties of trimethylammonium tetrachlorocobaltate crystals, *Phase transitions*, 54, 131-136(1995).
doi:10.1080/01411599508213224
- Kasano, H., Takashige, M. and Mashiyama, H., J., Structure study of paraelectric-ferroelectric transition in Monoclinic K_2ZnBr_4 , *Phys. Soc. Jpn.*, 61(5), 1580 - 1584(1992).
doi:10.1143/JPSJ.61.1580
- Mashiyama, H., Hasebe, K. and Tanisaki, S., X – ray diffraction study on the incommensurate – commensurate phase transitions in $\{\text{N}(\text{CH}_3)_4\}_2\text{CoCl}_4$, *J. Phy. Soc. Jpn.*, 49(4), Suppl. B, 92(1980).
doi:10.1143/JPSJ.49.1633
- Mohanraj, V., P. Sakthivel, S. Ponnuswamy, P. Muthuraja, Dhandapani, M., *Materials Today: Proceedings* 8 (2019a) 1–10
- Mohanraj, V., Pavithra, R., Thenmozhi, M. and Umarani, R., Synthesis, spectral, structural and thermal characterization of inorganic crystal : Phenyl trimethylammonium tetrachlorocobaltate, *Asian J. Chem.*, 31(8), 1779-1784(2019b).
doi:10.14233/ajchem.2019.21929
- Peer Mohamed, M., Sudha, C., Jayaprakash, P., Vinitha, G., Nageswari, M., Sangeetha, P., Rathika ThayaKumari, C. and Lydia Caroline, M., Growth and characterization of L-histidinium fumarate fumaric acid monohydrate single crystal: A promising second and third order non linear optical material, *Chinese J Phys*, 60, 581-597(2019).
doi:10.1016/j.cjph.2019.05.032
- Sannikov, D. G. and Lavanyak, A. P., ‘Incommensurate Phases in Dielectrics’ 2, Elsevier Science publisher, 43(1986).
- Sato, S., Ikeda, R. and Nakamura, D., Motions of tetramethylammonium cations and phase transitions in solid $[(\text{CH}_3)_4\text{N}]_2\text{CdX}_4$ ($\text{X} = \text{Cl, Br, I}$) as studied by ^1H NMR, powder X-ray

diffraction and differential thermal analysis measurements, *Bull. Chem. Soc. Japan*, 59(6), 1981 (1986).

[doi:10.1246/bcsj.59.1981](https://doi.org/10.1246/bcsj.59.1981)

Sawada, S., Shiroshi, Y., Yamamoto, A., Takashige, M. and Mantuso, M., Ferroelectricity in $\{N(CH_3)_4\}_2 CoCl_4$, *Physics Letters A.*, 67(1), 56-58(1978).

[doi:10.1016/0375-9601\(78\)90566-2](https://doi.org/10.1016/0375-9601(78)90566-2)

Shimomura, S., Fujii, Y. and Hamaya, N., Hydrostatic pressure effect on the ferroelastic monoclinic phase of $[N(CH_3)_4]_2MCl_4$ (M = Fe, Zn), *Journal of the Physical Society of Japan*, 64(12), 4759(1995).

[doi:10.1143/JPSJ.64.4759](https://doi.org/10.1143/JPSJ.64.4759)

Subashini, R. and Arjun, S., Synthesis and physicochemical properties of bis(L-asparaginato) zinc (II): A promising new semiorganic crystal with high laser damage threshold for shorter wavelength generation, *Optics and Laser Technology*, 101, 248-256(2018).

[doi:10.1016/j.optlastec.2017.11.009](https://doi.org/10.1016/j.optlastec.2017.11.009)

Young Kim, D., Kwan, S. and GulYoon, J., *Physical Review B*, 57, No. 18, 1173 (1998).

Strukov, B. A., Global hysteresis in ferroelectrics with incommensurate phases, *Phase Transitions*, 15(2-3), 143-179(1989).

[doi:10.1080/01411598908206844](https://doi.org/10.1080/01411598908206844)